SOS-MUSIC, a subspace approach for EEG source imaging promoting sparsity of active sources

Carla Joud, Laurent Albera, Isabelle Merlet, Julie Coloigner

SOS-MUSIC, a subspace approach for EEG source imaging promoting sparsity of active sources

Carla Joud
Univ Rennes, INSERM
LTSI-UMR 1099
Univ Rennes, INRIA
CNRS, IRISA, INSERM
Empenn U1228 ERL
carla.joud@irisa.fr

Laurent Albera
Univ Rennes, INSERM
LTSI-UMR 1099
F-35000, Rennes, France
laurent.albera@univ-rennes.fr

Isabelle Merlet
Univ Rennes, INSERM
LTSI-UMR 1099
F-35000, Rennes, France
isabelle.merlet@univ-rennes.fr

Julie Coloigner
Univ Rennes, INRIA
CNRS, IRISA, INSERM
Empenn U1228 ERL
F-35000, Rennes, France
julie.coloigner@irisa.fr

***Abstract*—Localizing multiple synchronous brain current sources from ElectroEncephaloGraphy (EEG) recordings is a challenging problem in presurgical evaluation of certain diseases such as drug resistant epilespy. In this paper, we propose a novel MUSIC-like (MUltiple SIgnal Classification) EEG source imaging method, named SOS-MUSIC. The latter minimizes the MUSIC metric as well as promoting Sparsity Of active Sources (SOS) to enhance performance. Indeed, by this way SOS-MUSIC helps to deal with synchronous (i.e. totally correlated) brain current sources, unlike classical approaches. This is illustrated through realistic computer simulations in the context of epilepsy by analyzing two challenging situations (low signal-to-noise ratios or correlated brain sources).**

***Index Terms*—EEG source imaging, MUSIC, sparsity, synchronous sources.**

I. Introduction

ElectroEncephaloGraphy (EEG) is used to measure the electric potential differences generated by neuronal activity at the surface of the head. It can be utilized for the localization and reconstruction of brain current sources, well-known as the EEG Source Imaging (ESI) problem [1], [2]. ESI is increasingly used in the clinic. For instance, performing ESI of interictal and ictal epileptic activity has become an useful diagnostic tool in presurgical epilepsy evaluation [3].

Two categories of ESI methods have been developed [4]: parametric versus non-parametric methods. The first category approach considers that few isolated dipoles represent the brain current sources of interest. For non-parametric approaches, also referred to as distributed sources methods, each brain current source of interest is characterized by a large number of dipoles, which are distributed in the brain volume or cortical surface. In the latter context, ESI requires supplementary assumptions to solve the underlying ill-posed inverse problem [5], [6].

One of the most famous non-parametric methods is the weighted Minimum Norm Estimate (wMNE) based on Tikhonov regularization [7]. Sparse priors were also used leading to probabilistic techniques [8] and deterministic ones such as the well-known Minimum current estimate (MCE) [9]. Regarding the parametric methods, they can be classified into three types: dipole fitting approaches [10], beamforming techniques [11] and subspace methods such as the Multiple Signal Classification (MUSIC) algorithm [12]. MUSIC-like techniques compute a noise subspace from the recorded EEG data, which is orthogonal to the signal subspace spanned by the leadfield vectors of the brain current sources of interest. Several variants aiming at improving the performance of the original MUSIC method have been proposed such as the Recursive MUSIC (R-MUSIC) algorithm [13], fourth order MUSIC-like methods (4-MUSIC) [14], and higher order sequential MUSIC-like techniques ($2q$-RapMUSIC and $2q$-D-MUSIC) [15]. However, despite of their great interests, these methods give a poor performance when trying to localize synchronous (i.e. totally correlated) brain current sources.

In order to overcome this drawback, in this paper we propose the SOS-MUSIC method, which minimizes the MUSIC metric while promoting Sparsity Of the active Sources (SOS). Due to the use of the L_1 norm, the underlying cost function is non-differentiable. Then, the ISTA proximal algorithm is implemented to minimize it. The computation of an optimal stepsize is provided in order to accelerate its convergence. Finally, we analyse the performance of SOS-MUSIC compared with MUSIC, 4-MUSIC and MCE through computer simulations in the context of epilepsy.

The formulation of the ESI problem and some assumptions are given in Section II. Then, the SOS-MUSIC method is presented in Section III. Performance results obtained from computer simulations are provided in Section IV. Eventually a conclusion and some perspectives are given in Section V.

II. Assumptions and problem formulation

We assume that T independent realizations of an N-dimensional random vector $\boldsymbol{x}$ are observed, leading to the recorded EEG data matrix $\boldsymbol{X}$ of size $(N \times T)$. By solving the forward problem [16], we have:

$$\boldsymbol{x} = \boldsymbol{G}(\Theta)\boldsymbol{s} = \sum_{p=1}^{P} \boldsymbol{g}(\theta_p)\, s_p \tag{1}$$

where $\boldsymbol{s}$ is a P-dimensional random vector, which realizations are the time courses of P current dipoles lining the brain

surface. The $(N \times P)$ matrix $\boldsymbol{G}(\Theta) = [\boldsymbol{g}(\theta_1), \cdots, \boldsymbol{g}(\theta_P)]$ is the so-called leadfield matrix, which characterizes the propagation of the cortical electric field towards the scalp electrodes. Given a head model and a source space, $\boldsymbol{G}(\Theta)$ can be computed by solving numerically Poisson's equation [16] by means of the Boundary Element Method (BEM) [17]. Without loss of generality, the N-dimensional random vector $\boldsymbol{x}$ is assumed to be zero mean. By assuming that few isolated dipoles represent the brain current sources of interest, the model (1) can be rewritten as follows:

$$\boldsymbol{x} = \sum_{p=1}^{P^{(e)}} \boldsymbol{g}(\theta_{\sigma(p)})\, s_{\sigma(p)} + \sum_{p=P^{(e)}+1}^{P} \boldsymbol{g}(\theta_{\sigma(p)})\, s_{\sigma(p)} \qquad (2)$$

where $P^{(e)}$ and σ denote the number of epileptic brain current sources and a permutation of the set $\{1, 2, \cdots, P\}$, respectively. The permutation is used to reorder epileptic sources in the first $P^{(e)}$ indices. In practice, the $P - P^{(e)}$ non-epileptic brain current sources, named background sources, are considered as a noise, hence the following model:

$$\boldsymbol{x} = \boldsymbol{G}(\Theta^{(e)})\, \boldsymbol{s}^{(e)} + \boldsymbol{n} \qquad (3)$$

where $\boldsymbol{G}(\Theta^{(e)}) = [\boldsymbol{g}(\theta_{\sigma(1)}), \cdots, \boldsymbol{g}(\theta_{\sigma(P^{(e)})})]$, $\boldsymbol{s}^{(e)} = [s_{\sigma(1)}, \cdots, s_{\sigma(P^{(e)})}]$ and $\boldsymbol{n}$ stand for the $(N \times P^{(e)})$ full column rank static mixing matrix, the $P^{(e)}$-dimensional random vector of the epileptic sources and the N-dimensional background noise random vector statistically independent of the epileptic sources, respectively. For the sake of convenience, the matrices $\boldsymbol{G}(\Theta)$ and $\boldsymbol{G}(\Theta^{(e)})$ will be denoted by $\boldsymbol{G}$ and $\boldsymbol{G}^{(e)}$, respectively, in the sequel.

III. The SOS-MUSIC method

This section recalls the principle of MUSIC which requires that the number $P^{(e)}$ of epileptic sources is strictly lower than the number N of electrodes. In practice, this number of targeted sources is determined using model selection informed by theorical criteria. Wax and Kailath were the first to address this problem by minimizing the AIC and MDL criteria [18]. Next the SOS-MUSIC method is presented in detail.

A. The MUSIC metric

MUSIC, as all the subspace approaches, consists in exploiting the orthogonality between a noise subspace $\mathcal{E}_n$ of dimension $N - P^{(e)}$ derived from some statistics of the data and the $P^{(e)}$-dimensional signal subspace $\mathcal{E}_s = \mathrm{span}(\boldsymbol{G}^{(e)})$ spanned by the column vectors of $\boldsymbol{G}^{(e)}$. As a consequence, the Euclidean inner product of each column vector of $\boldsymbol{G}^{(e)}$ and any vector of $\mathcal{E}_n$ is equal to zero. Thus the following MUSIC metric can be easily derived by i) computing the Euclidean inner product of one leadfield vector $\boldsymbol{g}$ of $\boldsymbol{G}$ and $N - P^{(e)}$ basis vectors $\boldsymbol{e}_m$ of $\mathcal{E}_n$, ii) summing the squares of these $N - P^{(e)}$ Euclidean inner products and iii) normalizing the latter sum:

$$\Upsilon(\boldsymbol{g}) = \frac{\sum_{m=1}^{N-P^{(e)}} (\langle \boldsymbol{g}, \boldsymbol{e}_m \rangle)^2}{\sum_{i=1}^{P^{(e)}} (g_i)^2} = \frac{||\boldsymbol{g}^\intercal \boldsymbol{E}_n||_2^2}{||\boldsymbol{g}||_2^2} = \frac{\boldsymbol{g}^\intercal \boldsymbol{E}_n \boldsymbol{E}_n^\intercal \boldsymbol{g}}{\boldsymbol{g}^\intercal \boldsymbol{g}} \qquad (4)$$

with $\boldsymbol{E}_n = [\boldsymbol{e}_1, \cdots, \boldsymbol{e}_{N-P^{(e)}}]$. In practice, the basis vectors $\boldsymbol{e}_m$ of $\mathcal{E}_n = \mathrm{span}(\boldsymbol{E}_n)$ are computed as the eigenvectors associated with the $N - P^{(e)}$ lowest eigenvalues of the covariance matrix $\boldsymbol{R}_{\boldsymbol{x}}$ of $\boldsymbol{x}$. The leadfield vectors of the $P^{(e)}$ epileptic sources are thus identified by scanning each column vector $\boldsymbol{g}$ of the leadfield matrix $\boldsymbol{G}$ and by keeping those which correspond to global minimizers of Υ (4).

B. The SOS-MUSIC approach

In this section, we present the SOS-MUSIC method based on i) the MUSIC metric defined in (4) and ii) a sparsity constraint on active sources, which avoids the time-consuming scanning procedure of MUSIC and allows for an efficient localization of synchronous epileptic sources.

As explained above, function Υ (4) has at least $P^{(e)}$ global minimizers given by the leadfield vectors of the $P^{(e)}$ epileptic sources. But more generally, since the signal subspace $\mathcal{E}_s = \mathrm{span}(\boldsymbol{G}^{(e)})$ and the noise subspace $\mathcal{E}_n$ are orthogonal complements of $\mathbb{R}^N$, the nonnegative MUSIC metric Υ is zero if and only if its argument is a linear combination $\boldsymbol{z}^{(e)} \in \mathbb{R}^N$ of column vectors of matrix $\boldsymbol{G}^{(e)}$. It is noteworthy that such a vector $\boldsymbol{z}^{(e)}$ can be decomposed as $\boldsymbol{G}\boldsymbol{v}^{(e)}$ where $\boldsymbol{v}^{(e)} \in \mathbb{R}^P$ is a sparse vector whose non-zero components select and weight the column vectors of $\boldsymbol{G}$ corresponding to column vectors of $\boldsymbol{G}^{(e)}$. Then, finding such a $P^{(e)}$-sparse vector $\boldsymbol{v}^{(e)}$, will allow us to find the leadfield vectors of the $P^{(e)}$ epileptic sources. Consequently, the ESI problem can be refmormulated as the following global minimization over the set of $P^{(e)}$-sparse vectors:

$$\min_{\boldsymbol{v} \in \mathbb{R}^P} \Upsilon(\boldsymbol{G}\boldsymbol{v}) + \lambda ||\boldsymbol{v}||_1 \qquad (5)$$

An appropriate selection of the penalty parameter λ will enforce the $P^{(e)}$-sparsity of the solution. For solving (5), we decided to use the Iterative Soft Thresholding Algorithm (ISTA) [19]. This efficient optimization algorithm allows for the minimization of non-differentiable cost functions involving the L_1 norm, especially for solving large-scale problems. Using ISTA, the update rule of $\boldsymbol{v}$ is given by:

$$\boldsymbol{v}^{(k+1)} = \mathrm{S}_{\lambda t^{(k)}}(\boldsymbol{v}^{(k)} - t^{(k)} \nabla \Upsilon(\boldsymbol{G}\boldsymbol{v}^{(k)})) \qquad (6)$$

where $t^{(k)}$ is an appropriate stepsize and $\tau_\alpha : \mathbb{R}^D \to \mathbb{R}$ is the shrinkage operator defined by $\mathrm{S}_\alpha(\boldsymbol{v})_i = (|v_i| - \alpha)_+ \mathrm{sgn}(v_i)$, say the proximal operator of the L_1 norm. The gradient of function Υ with respect to $\boldsymbol{v}$ is given by:

$$\nabla \Upsilon(\boldsymbol{G}\boldsymbol{v}) = \frac{2}{(\boldsymbol{v}^\intercal \boldsymbol{G}^\intercal \boldsymbol{G}\boldsymbol{v})} [(\boldsymbol{G}^\intercal \boldsymbol{E}_n \boldsymbol{E}_n^\intercal \boldsymbol{G}\boldsymbol{v}) - \Upsilon(\boldsymbol{G}\boldsymbol{v})(\boldsymbol{G}^\intercal \boldsymbol{G}\boldsymbol{v})] \qquad (7)$$

Now we propose to calculate the optimal stepsize $t^{(k)}$, which minimizes $\Upsilon(\boldsymbol{v}^{(k)} - t \nabla \Upsilon(\boldsymbol{G}\boldsymbol{v}^{(k)}))$ with respect to t. Since the minimum value of Υ is equal to zero, it corresponds also to the zero of the numerator of Υ. Note that the numerator of Υ is nonnegative. Then, the zero of the numerator of Υ can be computed by minimizing the numerator Υ, say by vanishing the derivative of the numerator of $\Upsilon(\boldsymbol{v}^{(k)} - t \nabla \Upsilon(\boldsymbol{G}\boldsymbol{v}^{(k)}))$ with respect to t. It is noteworthy that the numerator of Υ is a

Algorithm 1 The SOS-MUSIC algorithm

Input: $P^{(e)}$, *tol*, *IterMax*, $\boldsymbol{X} \in \mathbb{R}^{N \times T}$, $\boldsymbol{G} \in \mathbb{R}^{N \times P^{(e)}}$

Orthogonalization from the singular value decomposition of $\boldsymbol{G}$: $\tilde{\boldsymbol{G}} = \boldsymbol{\Sigma}^{-1}\boldsymbol{U}^\top\boldsymbol{G}$ and $\tilde{\boldsymbol{X}} = \boldsymbol{\Sigma}^{-1}\boldsymbol{U}^\top\boldsymbol{X}$ from $\boldsymbol{G} = \boldsymbol{U}\boldsymbol{\Sigma}\boldsymbol{V}^\top$
Computation of $\hat{\boldsymbol{R}}_{\tilde{\boldsymbol{x}}} = (1/T)\tilde{\boldsymbol{X}}\tilde{\boldsymbol{X}}^\top$, an estimate of $\boldsymbol{R}_{\tilde{\boldsymbol{x}}}$
Eigenvalue decomposition of $\hat{\boldsymbol{R}}_{\tilde{\boldsymbol{x}}}$
Estimation of the noise eigenmatrix $\boldsymbol{E}_n$ corresponding to the eigenvectors related to the $N - P^{(e)}$ lowest eigenvalues of $\hat{\boldsymbol{R}}_{\tilde{\boldsymbol{x}}}$
Computation of $\boldsymbol{v}^{(0)}$ using a multi-initialisation procedure
for $k = 1$: IterMax **do**
  Compute the gradient $\nabla\Upsilon$ according to eq. (7)
  Compute $t^{(k+1)}$ according to eq. (8)
  Compute $\boldsymbol{v}^{(k+1)}$ according to eq. (6)
  if Stopping criteria $\leq$ *tol* **then**
    break
  end if
end for
return The indexes of the $P^{(e)}$ largest components of $\boldsymbol{v}^{(k+1)}$

second degree polynomial. This yields to the following update rule of t:

$$t^{(k)} = \frac{\nabla\boldsymbol{\Upsilon}(\boldsymbol{G}\boldsymbol{v}^{(k)})^\top\boldsymbol{G}^\top\boldsymbol{E}_n\boldsymbol{E}_n^\top\boldsymbol{G}\boldsymbol{v}^{(k)}}{\nabla\Upsilon(\boldsymbol{G}\boldsymbol{v}^{(k)})^\top\boldsymbol{G}\boldsymbol{E}_n\boldsymbol{E}_n\Upsilon_\nu{}^\top\boldsymbol{G}\nabla\Upsilon(\boldsymbol{G}\boldsymbol{v}^{(k)})} \quad (8)$$

In the initial steps of the algorithm, we enhance the matrix conditioning of $\boldsymbol{G}$ by multiplying it on the left by a matrix derived from its singular value decomposition, thereby improving the inverse problem resolution (see Algorithm 1). We propose also to use a multi-initialization to compute the initial vector $\boldsymbol{v}^{(0)}$, to facilitate the guidance through a global minimum and to avoid a local minimum due to the non-convexity of the function Υ. It consists of computing 50 random vectors $\boldsymbol{v}^{(0)}$ and selecting the one which minimizes the MUSIC metric after 25 iterations. Besides, we stop ISTA either when the number of iterations exceeds 1000 or when the relative difference of the measure $\Upsilon(\boldsymbol{G}\boldsymbol{v})$ between two successive iterations exhibits a value below a predefined threshold $tol = 10^{-4}$. The main steps of SOS-MUSIC are summarized in Algorithm 1.

IV. Results

In this section, the performance of the SOS-MUSIC algorithm is compared with that of two classical subspace methods, namely 2-MUSIC [12] and 4-MUSIC [14], and with that of the MCE technique [9]. Contrarily to 2-MUSIC, the 4-MUSIC approach does not compute the noise subspace from the covariance matrix. It derives it from the quadricovariance matrix, which brings together the fourth order cumulants of the data [20]. Regarding the MCE algorithm, it is a minimum norm approach assuming the spatial sparsity of the sources of interest.

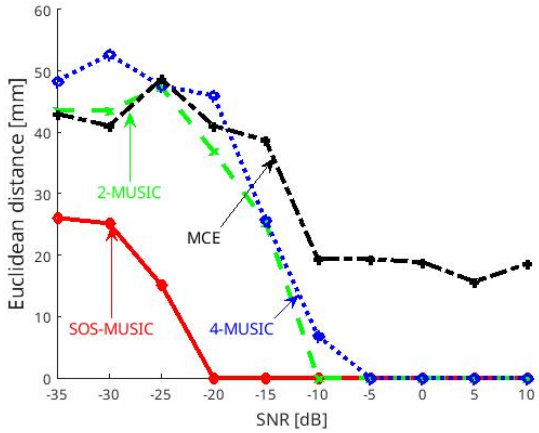

Fig. 1. Localization error in mm for one surface epileptic source

A. Data and performance criteria

The four methods were evaluated on 257 channels EEG data generated from a realistic model [21], which main features are briefly summarized below. A three-shell realistic head model was used including the brain, the skull and the scalp, whose conductivity are 0.33 $\Omega^{-1}m^{-1}$, 0.0082 $\Omega^{-1}m^{-1}$ and 0.33 $\Omega^{-1}m^{-1}$ respectively. The surfaces were extracted from the segmentation of the grey-white matter interface from a patient 3D T1-weighted MRI using Brain Visa software [22]. The source space consists of $P = 8000$ dipoles corresponding to the triangles of the cortical surface mesh with orientations perpendicular to the cortical surface. Each vertex of the mesh has been associated with an elementary current dipole. Using this realistic head model, the forward problem was solved using the Boundary Element Method (BEM) [17] to calculate the lead field matrix $\boldsymbol{G}$ of size (256×8000). The temporal dynamics of the activity of each dipole, were simulated using a computational neural mass model developed in our team for several years [23]. The parameters of this model can be adjusted to generate either background-like activity or interictal spikes. Dipoles that do not related to epileptic sources were attributed background activity with an amplitude that is adjusted to the amplitude of the epileptic spikes according to the given Signal-to-Noise Ratio (SNR) value.

All simulations are repeated for 10 Monte Carlo trials with different spike-like signals, background activities and source positions. The sources positions vary slightly, within 5mm of distance around the first source. The data are previously segmented around the spikes for reducing the noise. We keep around 300 time samples, by selecting few samples around all the observable epileptic spikes. The concatenation of these spike-like segments is given as input to the three MUSIC-like algorithms. When using these data in the MCE algorithm, the spike-like segments are averaged: MCE is applied to a specific time corresponding to the top of the averaged spike.

To evaluate the performance of the algorithms, we computed the Euclidean distance between the estimate source position

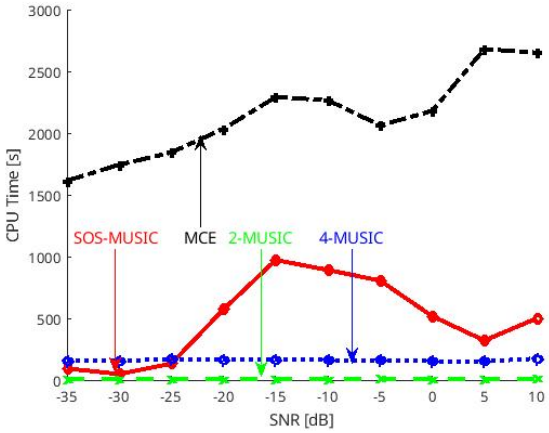

Fig. 2. CPU time in seconds for one surface epileptic source

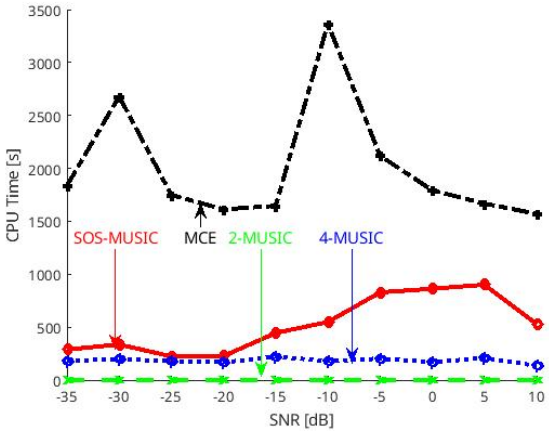

Fig. 4. CPU time in seconds for one deep epileptic source

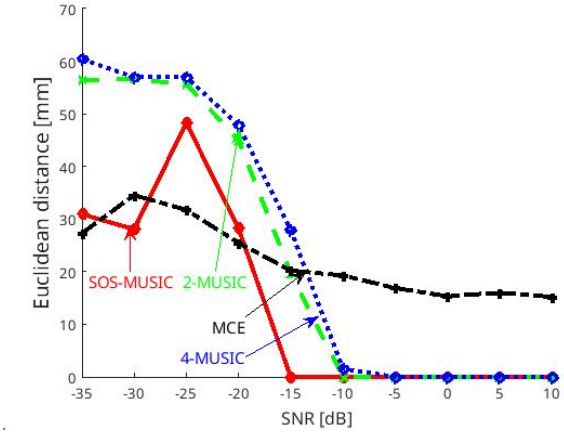

Fig. 3. Localization error in mm for one deep epileptic source

$(\hat{\theta}_i)$, and the true position (θ_i):

$$d_{\theta_i}^{\text{Euc}} = ||\hat{\theta}_i - \theta_i||_2 \tag{9}$$

Moreover, for large scale problems, the computational efficiency of the optimization algorithms used for minimization is important. Thus, we also used the CPU time as performance criterion to compare the fourth algorithms. It is noteworthy that the median of the two previous performance criteria was computed at the output of the four algorithms through two different scenarios: i) one epileptic source with a varying SNR value, and ii) two synchronous (i.e. totally correlated) epileptic sources for an SNR value of -5 dB.

B. Influence of the SNR value on source localization

Since EEG data is usually noisy, an important issue of source localization methods is their robustness with respect to noise. The behaviour of the four algorithms was studied in the presence of a unique epileptic source $P^{(e)} = 1$ for an SNR value ranging from -35 dB to 10 dB. The epileptic source is chosen by considering two different depths: a source localized on the surface of the cortex and a deep source.

Figures 1 and 3 show the Euclidean distance-based error (3) at the output of the four algorithms as a function of the SNR, in the case of one surface source (see Fig. 1) and in the case of one deep source (see Fig. 3). In both cases, it appears that for SNR values above -5 dB, the localization of the epileptic source is perfect ($d_{\theta_i}^{\text{Euc}} < 5$ mm) for SOS-MUSIC, 2-MUSIC and 4-MUSIC whereas MCE shows difficulty having a correct source localization. For SNR values below -10 dB, SOS-MUSIC appears to give a better location compared to the three other methods, whatever the considered depth. In other words, SOS-MUSIC seems to be more robust with respect to the presence of noise than the three other techniques. For very low SNR values (below -20 dB), for which the spike-like activity is completely drowned out by noise, we can see that all methods fail to localize the epileptic source. As described above, another way to differentiate the four algorithms is to compare their CPU times. Figures 2 and 4 display the CPU time (in seconds) at the ouptut of the four algorithms as a function of the SNR in the case of a surface source and a deep source, respectively. The SOS-MUSIC method appears to be at least two times faster than the MCE technique. Regarding the classical MUSIC-like methods, they give lower CPU times.

C. Incluence of the signal correlation on source localization

The SOS-MUSIC was designed in order to improve the source localization of synchronous (i.e. totally correlated sources), while the classical MUSIC-like methods are known to not be able to deal with such a practical case. Then, two synchronous epileptic sources were considered on the cortical surface (see Fig. 5). We fixed the SNR value to -5 dB.

Table I gives the sum of the two Euclidean distances and the CPU time computed at the output of the four methods. It clearly appears that 2-MUSIC, 4-MUSIC et MCE have difficulty in localizing the two sources, whereas SOS-MUSIC performs very well. As expected, the classical MUSIC-like

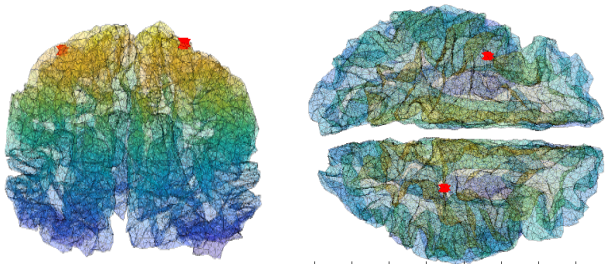

(a) Frontal wiew of the brain (b) Top wiew of the brain

Fig. 5. Location of the two considered synchronous epileptic sources

methods suffer from the correlation between the two sources. The SOS-MUSIC is more time-consuming than 2-MUSIC and 4-MUSIC while remaining cheaper than MCE.

TABLE I
LOCALIZATION ERROR AND CPU TIME IN THE PRESENCE OF TWO SYNCHRONOUS EPILEPTIC SOURCES WITH AN SNR VALUE OF -5 DB

Methods	Euclidean distance [mm]	CPU Times [s]
2-MUSIC	80.68	1.8
4-MUSIC	71.2	231.7
MCE	72.7	2540
SOS-MUSIC	0	710.7

V. DISCUSSION & CONCLUSION

In this paper, we proposed a novel MUSIC-like algorithm for brain current source localization, named the SOS-MUSIC approach. The latter minimizes the second-order MUSIC metric as well as promoting Sparsity Of the active Sources to enhance performance. Indeed, by this way SOS-MUSIC helps to deal with synchronous (i.e. totally correlated) brain current sources and low signal-to-noise ratios, unlike classical approaches, as demonstrated through realistic computer simulations. Although the SOS-MUSIC algorithm is more time-comsuming than the 2-MUSIC and 4-MUSIC methods, the results are more accurate. More complex simulation scenarios and comparisons of our approach with other methods are required to truly investigate this enhancement.

In this way, the next steps involve validating the developed algorithm on real EEG data. Following this, future works will consist in extending the SOS-MUSIC approach based on the second order MUSIC metric to higher order statistics, making it more robust with respect to the background noise, which is assumed Gaussian.

REFERENCES

[1] B. C. Cox, O. A. Danoun, B. N. Lundstrom, T. D. Lagerlund, L. C. Wong-Kisiel, and B. H. Brinkmann, "EEG source imaging concordance with intracranial EEG and epileptologist review in focal epilepsy," *Brain Communications*, vol. 3, no. 4, p. fcab278, 11 2021.

[2] Z. Yu, A. Kachenoura, R. L. B. Jeannès, H. Shu, P. Berraute, A. Nica, I. Merlet, L. Albera, and A. Karfoul, "Electrophysiological brain imaging based on simulation-driven deep learning in the context of epilepsy," *NeuroImage*, vol. 285, p. 120490, 2024.

[3] V. Brodbeck, L. Spinelli, A. M. Lascano, M. Wissmeier, M.-I. Vargas, S. Vulliemoz, C. Pollo, K. Schaller, C. M. Michel, and M. Seeck, "Electroencephalographic source imaging: a prospective study of 152 operated epileptic patients," *Brain*, vol. 134, no. 10, pp. 2887–2897, 09 2011.

[4] R. Grech, T. Cassar, J. Muscat, K. P. Camilleri, S. G. Fabri, M. Zervakis, P. Xanthopoulos, V. Sakkalis, and B. Vanrumste, "Review on solving the inverse problem in eeg source analysis," *Journal of NeuroEngineering and Rehabilitation*, vol. 5, no. 25, 2008.

[5] R. Pascual-Marqui, C. Michel, and D. Lehmann, "Low resolution electromagnetic tomography: a new method for localizing electrical activity in the brain," *International Journal of Psychophysiology*, vol. 18, no. 1, pp. 49–65, 1994.

[6] H. Becker, L. Albera, P. Comon, R. Gribonval, F. Wendling, and I. Merlet, "Brain-source imaging: From sparse to tensor models," *IEEE Signal Processing Magazine*, vol. 32, no. 6, pp. 100–112, 2015.

[7] M. Hämäläinen and R. Ilmoniemi, "Interpreting magnetic fields of the brain: minimum norm estimates," *Med. Biol. Eng. Comput.*, vol. 32, pp. 35–42, 1994.

[8] F. Costa, H. Batatia, L. Chaari, and J.-Y. Tourneret, "Sparse eeg source localization using bernoulli laplacian priors," *IEEE Transactions on Biomedical Engineering*, vol. 62, no. 12, pp. 2888–2898, 2015.

[9] K. Uutela, M. Hämäläinen, and E. Somersalo, "Visualization of magnetoencephalographic data using minimum current estimates," *Neuroimage*, vol. 10, no. 2, pp. 173–180, August 1999.

[10] M. Scherg and D. Von Cramon, "Evoked dipole source potentials of the human auditory cortex," *Electroencephalography and Clinical Neurophysiology/Evoked Potentials Section*, vol. 65, p. 344–360, 1986.

[11] Y. Jonmohamadi, G. Poudel, C. Innes, D. Weiss, R.Krueger, and R. Jones, "Comparison of beamformers for EEG source signal reconstruction," *Biomedical Signal Processing and Control*, vol. 14, no. 1, pp. 175–1888, 2014.

[12] R. O. Schmidt, "Multiple emitter location and signal parameter estimation," *IEEE Transactions On Antennas Propagation*, vol. 34, no. 3, pp. 276–280, March 1986, reprint of the original 1979 paper from the RADC Spectrum Estimation Workshop.

[13] J. C. Mosher and R. M. Leahy, "Recursive music: A framework for eeg and meg source localization," *IEEE Transactions On Biomedical Engineering*, vol. 45, no. 11, pp. 1342–1354, November 1998.

[14] L. Albera, A. Ferreol, D. Cosandier-Rimele, I. Merlet, and F. Wendling, "Brain source localization using a fourth-order deflation scheme," *IEEE Transactions on Biomedical Engineering*, vol. 55, no. 2, pp. 490–501, 2008.

[15] G. Birot, L. Albera, and P. Chevalier, "Sequential high-resolution direction finding from higher order statistics," *IEEE Transactions on Signal Processing*, vol. 58, no. 8, pp. 4144–4155, 2010.

[16] H. Hallez, B. Vanrumste, R. Grech, J. Muscat, W. D. Clercq, and A. V. et al., "Review on solving the forward problem in EEG source analysis," *Journal of NeuroEngineering and Rehabilitation*, vol. 4, no. 46, November 2007.

[17] A. Gramfort, T. Papadopoulo, E. Olivi, and M.Clerc, "OpenMEEG: Opensource software for quasistatic bioelectromagnetics," *BioMedical Engineering Online*, vol. 9, no. 1, p. 45, September 2012.

[18] M. wax and T. Kailath, "Detection of signals by information theoretic criteria," *IEEE Transactions on Acoustic, Speech and Signal Processing*, vol. 33, no. 2, pp. 387–392, April 1985.

[19] I. Daubechies, M. Defrise, and C. D. Mol, "An iterative thresholding algorithm for linear inverse problems with a sparsity constraint," *Comm. Pure Appl. Math.*, vol. 57, pp. 1413–1457, November 2004.

[20] P. McCullagh, *Tensor Methods in Statistics*. Chapman and Hall, Monographs on Statistics and Applied Probability, 1987.

[21] D. Cosandier-Rimélé, I. Merlet, J. Badier, P. Chauvel, and F. Wendling, "The neuronal sources of eeg: Modeling of simultaneous scalp and intracerebral recordings in epilepsy," *NeuroImage*, vol. 42, no. 1, pp. 135–146, 2008.

[22] D. Rivière, D.Geffroy, I. Denghien, N. Souedet, and Y. Cointepas, "BrainVISA: An extensible soft software environment for sharing multimodal neuroimaging data and processing tools," *B15th HBM*.

[23] F. Wendling, A. Hernandez, J. J. Bellanger, P.Chauvel, and F.Bartolomei, "Interictal to ictal transition in human temporal lobe epilepsy: Insights from a computational model of intracerebral eEG," *Journal of Clinical Neurophysiology*, vol. 22, no. 5, pp. 343–356, October 2005.